Ternary Scandium-rich Indides $Sc_{50}T_{13}In_3$ and $Sc_{50}Rh_{13}In_3O_y$ (T = Rh, Ir; $y \approx 8$) – Synthesis and Crystal Structure

Roman Zaremba and Rainer Pöttgen

Institut für Anorganische und Analytische Chemie, Universität Münster, Corrensstraße 30, D-48149 Münster, Germany

Reprint requests to R. Pöttgen. E-mail: pottgen@uni-muenster.de

Z. Naturforsch. **2007**, *62b,* 1567 – 1573; received August 31, 2007

New intermetallic compounds $Sc_{50}Rh_{13.3}In_{2.7}$ and $Sc_{50}Ir_{13.6}In_{2.4}$ and the suboxides $Sc_{49.2}Rh_{13}In_{3.8}O_{8.8}$ and $Sc_{49.2}Rh_{13.7}In_{2.8}O_{8.0}$ were synthesized from the elements or with Sc_2O_3 as an oxygen source, respectively, in sealed tantalum tubes in a water-cooled sample chamber of an induction furnace. They crystallize with a new cubic structure type, space group $Fm\bar{3}$, a = 1772.5(6) pm, $wR2$ = 0.032, 1111 F^2 values, 34 variables for $Sc_{50}Rh_{13.3}In_{2.7}$, a = 1766.5(6) pm, $wR2$ = 0.041, 745 F^2 values, 34 variables for $Sc_{50}Ir_{13.6}In_{2.4}$, a = 1764.4(2) pm, $wR2$ = 0.044, 690 F^2 values, 41 variables for $Sc_{49.2}Rh_{13}In_{3.8}O_{8.8}$, and a = 1761.5(6) pm, $wR2$ = 0.054, 740 F^2 values, 42 variables for $Sc_{49.2}Rh_{13.7}In_{2.8}O_{8.0}$. The main structural motifs are rhodium-centered indium cubes in an *fcc* like arrangement in which the octahedral and tetrahedral voids are filled by $In2Sc_{12}$ and $In1Sc_{12}$ icosahedra, respectively, resembling a Li_3Bi-like structure. The Rh1 (Ir1) and Sc4 atoms lie between these polyhedral units. The oxygen atoms partially fill Sc_6 octahedra in $Sc_{49.2}Rh_{13}In_{3.8}O_{8.8}$ and $Sc_{49.2}Rh_{13.7}In_{2.8}O_{8.0}$ with Sc–O distances of 214 – 230 pm. These octahedra are condensed *via* common edges and faces, encapsulating the $In2Sc_{12}$ icosahedra. Due to the high scandium content one observes strong Sc–Sc bonding with Sc–Sc distances ranging from 303 to 362 pm in $Sc_{49.2}Rh_{13}In_{3.8}O_{8.8}$. The shortest distances occur for Sc–Rh (267 – 295 pm). The crystal chemical relationship with the Li_3Bi-related suboxide $Ti_{12}Sn_3O_{10}$ is discussed.

Key words: Scandium, Intermetallics, Suboxides, Crystal Structure

Introduction

Within the large family of rare earth (*RE*)-transition metal (*T*)-indides [1], those with scandium as rare earth metal component have only scarcely been investigated. So far, the indides $ScNi_4In$ ($MgCu_4Sn$-type) [2], ScT_2In (T = Ni, Cu, Pd, Ag, Pt, Au) ($MnCu_2Al$-type) [3 – 5], Sc_2T_2In (T = Ni, Cu, Pd, Au) (Mo_2FeB_2- or U_2Pt_2Sn-type) [6, 7], ScPtIn with ZrNiAl structure [8], $Sc_5Ni_2In_4$ and $Sc_5Rh_2In_4$ with $Lu_5Ni_2In_4$-type [9], the $Lu_3Co_{1.87}In_4$ related indides $Sc_3Ni_{2-x+y}In_{4-y}$ (x = 0.10, y = 0.24 and x = 0.30, y = 0.40), $ScPd_{0.981}In$ and $Sc_3Rh_{1.594}In_4$ [10], a solid solution $Sc_{1-x}PdIn_x$ [11] with CsCl structure, $ScCu_4In$, $Sc_6Co_{2.18}In_{0.82}$, and $Sc_{10}Ni_9In_{19.44}$ [12] have been reported. Due to the small size of scandium, these compounds often adopt superstructures or deformation variants of known rare earth structures.

In the course of our systematic studies of rare earth metal-rich indides $RE_xT_yIn_z$ we recently reported on the new indides $RE_{14}Rh_3In_3$ [13], $RE_3T_{2-x}In_x$ (T = Rh, Ir) [14], RE_4RhIn [15] and RE_4IrIn [16]. When searching for related scandium-rich compounds we obtained the indides $Sc_{50}Rh_{13.3}In_{2.7}$ and $Sc_{50}Ir_{13.6}In_{2.4}$, and the suboxides $Sc_{49.2}Rh_{13}In_{3.8}O_{8.8}$, and $Sc_{49.2}Rh_{13.7}In_{2.8}O_{8.0}$, which crystallize with a new structure type. The synthesis and crystal chemistry of these phases are reported herein.

Experimental Section

Synthesis

Starting materials for the synthesis of the scandium compounds were scandium ingots (Kelpin, > 99.9 %), rhodium and iridium powder (Heraeus, > 99.9 %), indium tear drops (Johnson Matthey, > 99.9 %), and Sc_2O_3 (Heraeus, > 99.9 %). First, the scandium ingots were cut into smaller pieces and arc-melted [17] to small buttons under an argon atmosphere. The argon was purified over titanium sponge (900 K), silica gel, and molecular sieves. The pre-melting procedure reduces shattering during the subsequent reactions with rhodium (iridium) and indium. The scandium buttons were then mixed with cold-pressed pellets (∅ 6 mm) of rhodium (iridium) and pieces of the indium tear drops in the

Table 1. Crystal data and structure refinement for $Sc_{50}Rh_{13.3(1)}In_{2.7(1)}$, $Sc_{50}Ir_{13.6(1)}In_{2.4(1)}$, $Sc_{49.2(1)}Rh_{13}In_{3.8(1)}O_{8.8(5)}$, and $Sc_{49.2(1)}Rh_{13.7(1)}In_{2.8(1)}O_{8.0(6)}$, space group $Fm\bar{3}$, $Z = 4$.

Empirical formula	$Sc_{50}Rh_{13.3}In_{2.7}$	$Sc_{50}Ir_{13.6}In_{2.4}$	$Sc_{49.2}Rh_{13}In_{3.8}O_{8.8}$	$Sc_{49.2}Rh_{13.7}In_{2.8}O_{8.0}$
Molar mass, g/mol	3927.19	5134.20	4126.75	4075.40
Unit cell dimensions, pm	a = 1772.5(6)	a = 1766.5(6)	a = 1764.4(2)	a = 1761.5(6)
(Guinier powder data), nm^3	V = 5.5688	V = 5.5124	V = 5.4928	V = 5.4657
Calculated density, g cm^{-3}	4.68	6.19	4.99	4.95
Crystal size, μm^3	$30 \times 110 \times 310$	$20 \times 70 \times 220$	$20 \times 70 \times 90$	$20 \times 30 \times 100$
Detector distance	–	–	100 mm	–
Exposure time	–	–	5 min	–
ω range; increment, deg	–	–	0 – 180; 1.0	–
Integr. param. A, B, EMS	–	–	16.1; 3.9; 0.029	–
Transm. ratio (max/min)	4.39	4.61	1.44	1.19
Absorption coefficient, mm^{-1}	10.5	39.2	10.9	10.8
$F(000)$	7124	8854	7499	7411
θ range, °	2 – 35	2 – 30	2 – 30	3 – 30
Range in hkl	±28, ±28, +28	−24/8, ±24, +24	±24, ±24, −22/24	±24, ±24, +24
Total no. reflections	12481	6020	13198	8253
Independent reflections	1111 (R_{int} = 0.099)	745 (R_{int} = 0.088)	690 (R_{int} = 0.069)	740 (R_{int} = 0.216)
Reflections with $I \geq 2\sigma(I)$	1025 (R_σ = 0.032)	652 (R_σ = 0.037)	518 (R_σ = 0.064)	479 (R_σ = 0.076)
Data/parameters	1111/34	745/34	690 / 41	740 / 42
Goodness-of-fit on F^2	1.178	1.102	0.773	1.005
Final R indices $[I \geq 2\sigma(I)]$				
$R1/wR2$	0.017/0.032	0.021/0.039	0.024 / 0.042	0.035 / 0.044
R indices (all data)				
$R1/wR2$	0.020/0.032	0.029/0.041	0.044 / 0.044	0.089 / 0.050
Extinction coefficient	0.00066(1)	0.000013(2)	0.000311(11)	0.000025(4)
Largest diff. peak and hole, e Å^{-3}	1.48/−1.30	1.65/−1.36	1.16/−1.77	1.90/−2.15

ideal 50 : 13 : 3 atomic ratio. The mixtures were reacted in tantalum tubes by induction melting in a water-cooled sample chamber of a high-frequency furnace (Hüttinger Elektronik, Freiburg, type TIG 2.5/300) under flowing argon [18]. The tubes were heated up to 1800 K, then slowly cooled to 1000 K at a rate of 130 K/h and kept at this temperature for ∼ 2 h, followed by quenching. The temperature was controlled through a Sensor Therm Methis MS09 pyrometer with an accuracy of ±30 K. For the syntheses of the oxides, an appropriate amount of scandium sesquioxide was used as oxygen source in the induction melting process with the same annealing sequence. The samples could easily be separated from the crucible material. No reaction with tantalum was observed. Polycrystalline samples are light grey while ground powders are dark grey. Single crystals exhibit metallic lustre. The compounds are stable in air.

X-Ray diffraction

The samples were characterized through Guinier powder patterns (imaging plate technique, Fujifilm BAS-1800) using Cu$K_{\alpha 1}$ radiation and α-quartz (a = 491.30 and c = 540.46 pm) as an internal standard. The lattice parameters (Table 1) were obtained from least-squares fits of the powder data. Correct indexing was ensured through a comparison of the experimental patterns with calculated ones [19], taking the atomic positions from the structure refinements.

Single crystal intensity data of the $Sc_{49.2}Rh_{13}In_{3.8}O_{8.8}$ crystal were collected at r. t. on a Stoe IPDS-II image plate system in oscillation mode. A numerical absorption correction was applied to the data set. The remaining crystals were measured on a four-circle diffractometer (CAD4) with graphite-monochromatized MoK_α radiation and a scintillation counter with pulse height discrimination. Scans were taken in the $\omega/2\theta$ mode. Empirical absorption corrections were applied on the basis of Ψ-scan data, accompanied by spherical absorption corrections. All relevant details concerning the data collections are listed in Table 1.

Structure refinements

Small, irregularly shaped single crystals of the four indides were selected from the annealed samples by mechanical fragmentation and examined by use of a Buerger camera equipped with an image plate system (Fujifilm BAS-1800) in order to establish suitability for intensity data collection. The data sets taken on the diffractometers showed only the systematic extinctions of cubic face-centered lattices, leading to the space groups $Fm\bar{3}m$, $Fm\bar{3}$, $F432$, and $F\bar{4}3m$, of which the centrosymmetric group $Fm\bar{3}$ was found to be correct during the structure refinements.

The starting atomic parameters were deduced from automatic interpretations of Direct Methods with SHELXS-97 [20] and the four structures were refined using SHELXL-

Table 2. Atomic coordinates and isotropic displacement parameters (pm^2) of $Sc_{50}Rh_{13.3(1)}In_{2.7(1)}$, $Sc_{50}Ir_{13.6(1)}In_{2.4(1)}$, $Sc_{49.2(1)}Rh_{13}In_{3.8(1)}O_{8.8(5)}$, and $Sc_{49.2(1)}Rh_{13.7(1)}In_{2.8(1)}O_{8.0(6)}$. U_{eq} is defined as one third of the trace of the orthogonalized U_{ij} tensor.

Atom	Wyckoff site	Occupancy (%)	x	y	z	U_{eq}
$Sc_{50}Rh_{13.3(1)}In_{2.7(1)}$						
Sc1	96*i*	100	0.09308(2)	0.25691(2)	0.15712(2)	93(1)
Sc2	48*h*	100	0	0.09294(2)	0.35499(2)	65(1)
Sc3	32*f*	100	0.08998(2)	*x*	*x*	65(1)
Sc4	24*e*	100	0.21216(3)	0	0	76(1)
Rh1	48*h*	100	0	0.15425(1)	0.21637(1)	119(1)
Rh2	4*a*	100	0	0	0	59(1)
In1	8*c*	100	1/4	1/4	1/4	78(1)
In2/Rh3	4*b*	74(2)/26(2)	1/2	1/2	1/2	58(1)
$Sc_{50}Ir_{13.6(1)}In_{2.4(1)}$						
Sc1	96*i*	100	0.09306(5)	0.25818(6)	0.15651(6)	77(2)
Sc2	48*h*	100	0	0.09127(7)	0.35667(7)	29(3)
Sc3	32*f*	100	0.09044(5)	*x*	*x*	37(3)
Sc4	24*e*	100	0.21248(11)	0	0	51(4)
Ir1	48*h*	100	0	0.15362(2)	0.21600(2)	85(1)
Ir2	4*a*	100	0	0	0	28(2)
In1	8*c*	100	1/4	1/4	1/4	48(2)
In2/Ir3	4*b*	44(1)/56(1)	1/2	1/2	1/2	45(4)
$Sc_{49.2(1)}Rh_{13}In_{3.8(1)}O_{8.8(5)}$						
Sc1	96*i*	100	0.09285(5)	0.25897(5)	0.15593(5)	62(2)
Sc2	48*h*	100	0	0.09102(7)	0.35677(7)	34(3)
Sc3/In3	32*f*	90.0(6)/10.0(6)	0.09085(4)	*x*	*x*	36(5)
Sc4	24*e*	100	0.21115(11)	0	0	41(4)
Rh1	48*h*	100	0	0.15532(3)	0.21517(3)	67(1)
Rh2	4*a*	100	0	0	0	37(4)
In1	8*c*	100	1/4	1/4	1/4	48(2)
In2	4*b*	100	1/2	1/2	1/2	57(3)
O1	32*f*	72(3)	0.3783(3)	*x*	*x*	105(28)
O2	48*h*	25(2)	0	0.1932(11)	0.4221(12)	68(64)
$Sc_{49.2(1)}Rh_{13.7(1)}In_{2.8(1)}O_{8.0(6)}$						
Sc1	96*i*	100	0.09255(7)	0.25882(7)	0.15620(7)	105(3)
Sc2	48*h*	100	0	0.09057(10)	0.35721(10)	77(4)
Sc3/In2	32*f*	89.7(6)/10.3(6)	0.09091(6)	*x*	*x*	91(6)
Sc4	24*e*	100	0.21116(15)	0	0	90(5)
Rh1	48*h*	97.6(4)	0	0.15514(5)	0.21521(5)	128(2)
Rh2	4*a*	100	0	0	0	108(6)
In1	8*c*	100	1/4	1/4	1/4	105(4)
Rh3	4*b*	100	1/2	1/2	1/2	88(5)
O1	32*f*	64(3)	0.3775(4)	*x*	*x*	147(41)
O2	48*h*	24(3)	0	0.1906(16)	0.4230(17)	201(103)

Table 3. Interatomic distances (pm), calculated with the powder lattice parameters of $Sc_{49.2(1)}Rh_{13}In_{3.8(1)}O_{8.8(5)}$. All distances within the first coordination spheres are listed. Standard deviations are equal or less than 0.2 pm for the metal-metal distances and 1.5 pm for the metal-oxygen distances. Note that the Sc3 position shows slight mixing with In3 (see Table 2).

Sc1:	1	O1	224.9	Sc2:	1	O2	214.0	Sc4:	2	O2	217.7	O1:	3	Sc2	224.7
	1	O2	230.0		2	O1	224.7		2	Rh1	274.2		3	Sc1	224.9
	1	Rh1	266.9		2	O2	229.1		2	Sc2	303.0	O2:	1	Sc2	214.0
	1	Rh1	306.3		1	Rh1	274.4		4	Sc3	310.6		1	Sc4	217.7
	1	Sc2	312.1		1	In2	299.4		4	Sc1	331.1		2	Sc2	229.0
	1	Sc3	318.1		1	Sc4	303.0	Rh1:	2	Sc1	266.9		2	Sc1	230.0
	1	Rh1	318.5		2	Sc1	312.1		1	Sc4	274.2				
	2	Sc1	321.4		4	Sc2	313.3		1	Sc2	274.4				
	1	In1	323.6		1	Sc2	321.2		2	Sc3	294.5				
	1	Sc2	324.8		2	Sc1	324.8		2	Sc1	306.3				
	1	Sc1	327.7	Sc3:	1	Rh2	277.6		2	Sc1	318.5				
	1	Sc4	331.1		3	Rh1	294.5	Rh2:	8	Sc3	277.6				
	1	Sc1	333.5		3	Sc4	310.6		6	Sc4	372.6				
	2	Sc1	362.4		3	Sc1	318.1	In1:	12	Sc1	323.6				
					3	Sc3	320.6	In2:	12	Sc2	299.4				

97 [21] (full-matrix least-squares on F^2) with anisotropic atomic displacement parameters for all metal atoms. The first crystal investigated revealed significant residual peaks of 9.9 and 3.2 e/Å^3 (well separated from other peaks), cor-

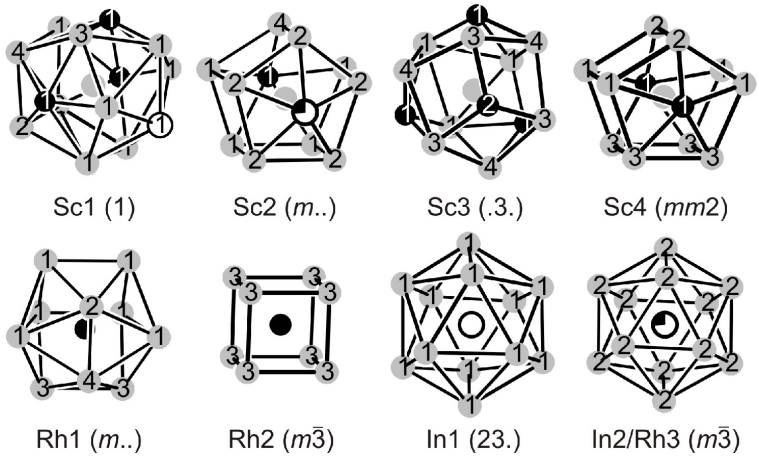

Fig. 1. Coordination polyhedra in the structure of $Sc_{50}Rh_{13.3}In_{2.7}$. Scandium, rhodium, and indium atoms are drawn as light grey, black, and open circles, respectively. Atom designations and site symmetries are given. The mixed occupied site is emphasized with segments.

responding to the Wyckoff sites 32*f* and 48*h*. These sites had octahedral scandium coordination with suitable Sc–O distances. In the following cycles two oxygen sites with free occupancy parameters were introduced. Later, a second oxygen-containing crystal (taken from a sample directly synthesized with Sc_2O_3 as an oxygen source) was refined with the same model (Table 2). Furthermore, for the two oxygen-free crystals In2/Rh3 and In2/Ir3 mixing on the 4*b* site was observed. The two suboxides revealed Sc3/In3 mixing on one 32*f* position. Furthermore, the $Sc_{49.2}Rh_{13.7}In_{2.8}O_{8.0}$ crystal showed small defects on the 48*h* Rh site, while the 4*b* site was exclusively filled by rhodium. The refined occupancy parameter for this position is 98(1) %. Thus, there is no indication for Rh/In mixing. The final difference Fourier syntheses were flat (Table 1). The positional parameters and interatomic distances (exemplarily for $Sc_{49.2}Rh_{13}In_{3.8}O_{8.8}$) of the refinements are listed in Tables 2 and 3.

Further details of the crystal structure investigations may be obtained from Fachinformationszentrum Karlsruhe, 76344 Eggenstein-Leopoldshafen, Germany (fax: +49-7247-808-666; e-mail: crysdata@fiz-karlsruhe.de, http://www.fiz-informationsdienste.de/en/DB/icsd/depot_anforderung.html) on quoting the deposition numbers CSD-418501 ($Sc_{50}Rh_{13.3}In_{2.7}$), CSD-418502 ($Sc_{50}Ir_{13.6}In_{2.4}$), CSD-418500 ($Sc_{49.2}Rh_{13}In_{3.8}O_{8.8}$), and CSD-418499 ($Sc_{49.2}Rh_{13.7}In_{2.8}O_{8.0}$).

Scanning electron microscopy

The bulk samples and the single crystals of the four scandium compounds investigated on the diffractometer were analyzed in a LEICA 420 I scanning electron microscope equipped with an OXFORD EDX analyzer. Since the crystals were mounted with varnish on glass fibres, they were first coated with a carbon film. Sc, Rh, Ir, and InAs were used as standards for the semiquantitative EDX measurements. The oxygen content could not be determined due to the detection limit of the instrument. The compositions (metals only) determined by EDX (75 ± 2 at.-% Sc : 20 ± 2 at.-% Rh : 5 ± 2 at.-% In for $Sc_{50}Rh_{13.3}In_{2.7}$, 76 ± 2 at.-% Sc : 19 ± 2 at.-% Ir : 5 ± 2 at.-% In for $Sc_{50}Ir_{13.6}In_{2.4}$, 74 ± 2 at.-% Sc : 20 ± 2 at.-% Rh : 6 ± 2 at.-% In for $Sc_{49.2}Rh_{13}In_{3.8}O_{8.8}$, and 74 ± 2 at.-% Sc : 21 ± 2 at.-% Rh : 5 ± 2 at.-% In for $Sc_{49.2}Rh_{13.7}In_{2.8}O_{8.0}$) are close to the ideal composition, *i. e.* 75.8 : 19.7 : 4.5. The standard uncertainties account for the analyses at various points. No impurity elements were observed.

Results and Discussion

The scandium-rich indides $Sc_{50}Rh_{13.3}In_{2.7}$, $Sc_{50}Ir_{13.6}In_{2.4}$, $Sc_{49.2}Rh_{13}In_{3.8}O_{8.8}$, and $Sc_{49.2}Rh_{13.7}In_{2.8}O_{8.0}$ crystallize with a new cubic structure type, space group $Fm\bar{3}$, with four formula units per cell. As an example we discuss the structures of $Sc_{50}Rh_{13.3}In_{2.7}$ and $Sc_{49.2}Rh_{13}In_{3.8}O_{8.8}$. The coordination polyhedra of the metal and oxygen atoms are shown in Figs. 1 and 2. The four crystallograph-

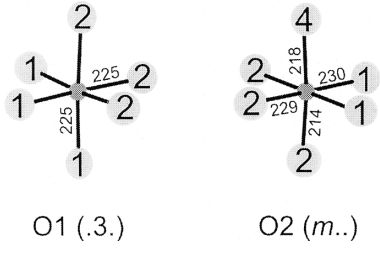

Fig. 2. Coordination of the oxygen atoms in the structure of $Sc_{49.2}Rh_{13}In_{3.8}O_{8.8}$. Scandium and oxygen atoms are drawn as light and medium grey circles, respectively. Atom designations, site symmetries, and relevant interatomic distances are given.

ically independent scandium atoms have coordination numbers between 12 and 14. The Sc2 and Sc4 atoms have the most symmetrical coordination polyhedra. They can be considered as pentagonal prisms which are capped on both pentagonal faces by rhodium or indium atoms (Fig. 1). The Sc3 atoms have four rhodium and nine scandium atoms in their coordination shell. The highest coordination number (CN 14) occurs for the Sc1 atoms.

The near-neighbor coordination for the two crystallographically independent rhodium atoms is completely different. The Rh1 atoms have the unusual CN 10, while the Rh2 atoms have a highly symmetric cubic coordination by Sc3 atoms. Usually observed is trigonal prismatic coordination for the rhodium atoms, *e. g.* in the series of $RE_{14}Rh_3In_3$ [13] and RE_4RhIn [15] compounds. The increase of the coordination number in the present compounds might be a result of the smaller size of scandium as compared to the larger rare earth elements. Both, In1 and the mixed occupied position In2/Rh3, have icosahedral scandium coordination.

The oxygen content was first detected in a sample prepared with presumably oxide contaminated scandium. In the following experiments, we used as much Sc_2O_3 as educt as would have been necessary for filling all of the octahedral voids. The two different coordination polyhedra for the 32*f* and 48*h* sites are presented in Fig. 2.

As expected for such a scandium-rich compound, we observe a broad range of Sc–Sc distances, *i. e.* 303 – 362 pm. Several Sc–Sc distances are shorter than the average Sc–Sc distance of 328 pm in *hcp* scandium [22] and we can safely assume strong Sc–Sc bonding in these cubic structures. The Sc–Sc distances are comparable to those in $Sc_5Rh_2In_4$ (323 – 371 pm) [9] and $Sc_3Rh_{1.594}In_4$ (342 – 367 pm) [10]. Significant Sc–Sc bonding has also been observed in the structures of ScNiP (323 – 373 pm) [23] and the scandium-rich tellurides Sc_6FeTe_2 (315 – 384 pm) [24], Sc_6AgTe_2 (305 – 359 pm) [25], and Sc_9Te_2 (300 – 362 pm) [26].

The shorter Sc–Rh distances range from 267 to 295 pm, close to the sum of the covalent radii [27] of 269 pm. Considering the electronegativity difference between scandium and rhodium, we can assume significant covalent Sc–Rh bonding in our indides. In contrast, the Sc–In distances are all longer than the sum of the covalent radii (294 pm) and the indium atoms do not belong to the first coordination sphere of the scandium atoms. The Sc–In interactions are weaker than the Sc–Rh ones.

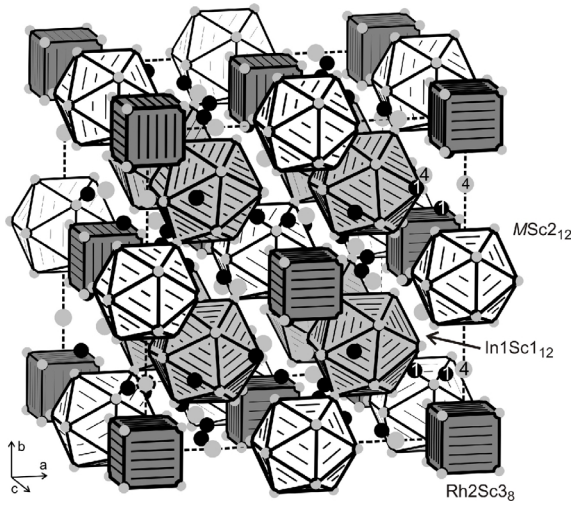

Fig. 3. Arrangement of the basic polyhedral units in the structure of $Sc_{50}Rh_{13.3}In_{2.7}$. Scandium, rhodium, and indium atoms are drawn as light grey, black, and open circles, respectively. The Rh1 and Sc4 atoms are not involved in these polyhedra. For details see text.

The structures contain two octahedral voids formed by the Sc1, Sc2, and Sc4 atoms. In two of our samples these voids are partially filled by oxygen (Table 2), resulting in Sc–O distances in the range from 214 to 230 pm. Comparable Sc–O distances occur in scandium phosphate framework structures [28], β-$CsSc(HAsO_4)_2$ [29] or microporous scandium terephthalate [30].

Topologically, the complex structure of $Sc_{50}Rh_{13.3}In_{2.7}$ is derived from the $MnCu_2Al$-type (ordered version of Li_3Bi) [31, 32] *via* a substitution of atoms by building groups. The Rh2Sc$_8$ cubes and the *M*Sc$_{12}$ icosahedra build up a rocksalt-like arrangement, similar to the manganese and aluminium atoms in the Heusler phase. The tetrahedral sites left by this arrangement (the copper sites of $MnCu_2Al$) are filled by the In1Sc$_{12}$ icosahedra (Fig. 3). This description *via* polyhedra considers all atoms with the exception of Sc4 and Rh1 which fill the space between these polyhedra. A similar topology has been observed for $Ti_{12}Sn_3O_{10}$ [33], *i. e.* Al $\Rightarrow$ TiO_8, Cu $\Rightarrow$ TiO_6, and Mn $\Rightarrow$ $TiSn_6$.

Fig. 4 emphasizes the coordination of the oxygen-centered Sc$_6$ octahedra. The In2Sc$_{12}$ icosahedra are connected to eight O1Sc$_6$ octahedra *via* common

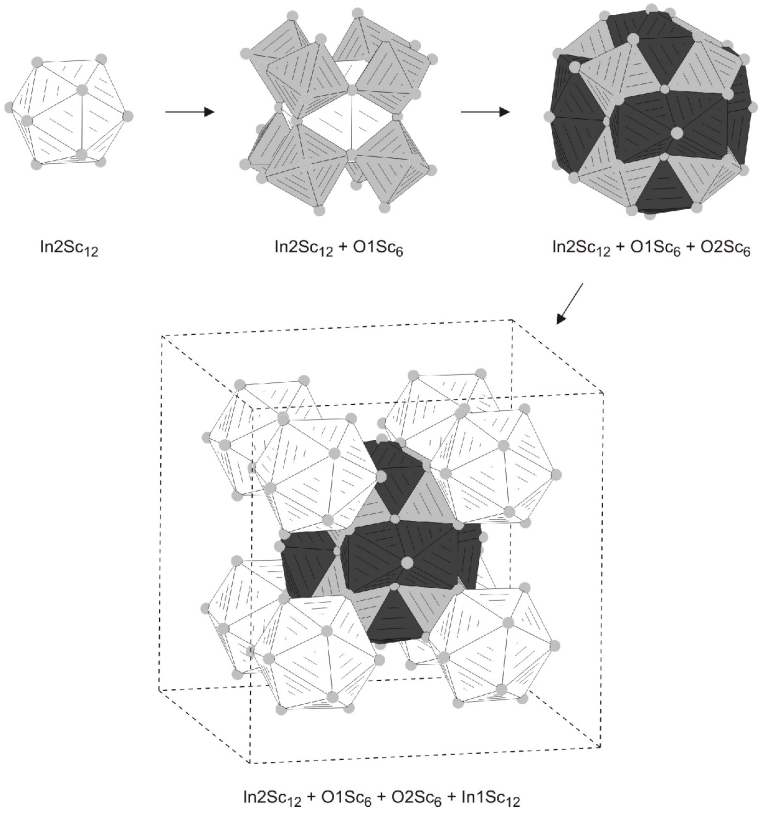

Fig. 4. The basic building units in the suboxide $Sc_{49.2}Rh_{13}In_{3.8}O_{8.8}$. For details see text.

edges. The $O1Sc_6$ octahedra build up a substructure that resembles the connectivity pattern of the $ReO_{6/3}$ octahedra in ReO_3, however, in a tilted fashion. In the second coordination sphere, the $In2Sc_{12}$ icosahedra are further connected to the $O2Sc_6$ octahedra *via* the remaining twelve faces. As emphasized in the upper right-hand part of Fig. 4, the oxygen-centered Sc_6 octahedra completely encapsulate the $In2Sc_{12}$ icosahedra. The octahedra share common faces. In both crystals investigated, all octahedra are only partially filled, including the sample with the highest initial oxygen content. In the next coordination sphere eight $In1Sc_{12}$ icosahedra connect to the larger ball *via* common triangular faces. Thus, the structure of $Sc_{49.2}Rh_{13}In_{3.8}O_{8.8}$ shows a separation into oxidic and intermetallic parts.

In the indium-based systems, an oxygen contamination has so far only been observed for the compounds $Gd_4IrInO_{0.25}$ and $Er_4IrInO_{0.25}$ [16] and the phases reported herein. The rare earth metal-rich phases leave enough octahedral voids which allow for oxygen incorporation. Since in both structural families the oxygen-free and the oxygen-containing species exist, both structure types have a certain flexibility in the electron count. Further investigations of the rare earth metal-rich parts of these phase diagrams are in progress in order to elucidate this rich and interesting crystal chemistry.

Acknowledgement

This work was financially supported by the Deutsche Forschungsgemeinschaft.

[1] Ya. M. Kalychak, V. I. Zaremba, R. Pöttgen, M. Lukachuk, R.-D. Hoffmann, in *Handbook on the Physics and Chemistry of Rare Earths*, Vol. 34, (Eds.: K. A. Gschneidner Jr., V. K. Pecharsky, J.-C. Bünzli), Elsevier, Amsterdam, **2005**, chapter 218.

[2] V. I. Zaremba, V. M. Baranyak, Ya. M. Kalychak, *Vestn. Lvov Univ., Ser. Khim.* **1984**, *25*, 18.

[3] N. N. Kiseleva, *Izv. Akad. Nauk. SSSR, Metally* **1987**, *2*, 213.

[4] A. E. Dwight, C. W. Kimball, *J. Less-Common Met*. **1987**, *127*, 179.
[5] B. T. Matthias, E. Corenzwit, J. M. Vandenberg, H. Barz, M. B. Maple, R. N. Shelton, *J. Less-Common Met*. **1976**, *46*, 339.
[6] R. Pöttgen, R. Dronskowski, *Z. Anorg. Allg. Chem*. **1996**, *622*, 355.
[7] F. Hulliger, *J. Alloys Compd*. **1996**, *232*, 160.
[8] Ya. V. Galadzhun, V. I. Zaremba, H. Piotrowski, P. Mayer, R.-D. Hoffmann, R. Pöttgen, *Z. Naturforsch*. **2000**, *55b*, 1025.
[9] M. Lukachuk, B. Heying, U. Ch. Rodewald, R. Pöttgen, *Heteroatom Chem*. **2005**, *16*, 364.
[10] M. Lukachuk, V. I. Zaremba, R.-D. Hoffmann, R. Pöttgen, *Z. Naturforsch*. **2004**, *59b*, 182.
[11] V. P. Urvachev, V. P. Polyakova, E. M. Savitskii in: *Splavy Redkikh Metallov s Osobymi Fizicheskimi Svojstvami: Redkozemelnye I. Blagorodnye Metally*, (Ed.: E. M. Savitskii), **1983**, 141.
[12] R. I. Zaremba, Ya. M. Kalychak, U. Ch. Rodewald, R. Pöttgen, V. I. Zaremba, *Z. Naturforsch*. **2006**, *61b*, 942.
[13] R. Zaremba, R. Pöttgen, *J. Solid State Chem*. **2007**, *180*, 2452.
[14] R. Zaremba, U. Ch. Rodewald, V. I. Zaremba, R. Pöttgen, *Z. Naturforsch*. **2007**, *62b*, 1397.
[15] R. Zaremba, U. Ch. Rodewald, R.-D. Hoffmann, R. Pöttgen, *Monatsh. Chem*. **2007**, *138*, 523.
[16] R. Zaremba, U. Ch. Rodewald, R.-D. Hoffmann, R. Pöttgen, *Monatsh. Chem*. **2007**, in press.
[17] R. Pöttgen, Th. Gulden, A. Simon, *GIT Labor-Fachzeitschrift* **1999**, 4*3*, 133.
[18] D. Kußmann, R.-D. Hoffmann, R. Pöttgen, *Z. Anorg. Allg. Chem*. **1998**, *624*, 1727.
[19] K. Yvon, W. Jeitschko, E. Parthé, *J. Appl. Crystallogr*. **1977**, *10*, 73.
[20] G. M. Sheldrick, SHELXS-97, Program for the Solution of Crystal Structures, University of Göttingen, Göttingen (Germany), **1997**.
[21] G. M. Sheldrick, SHELXL-97, Program for the Refinement of Crystal Structures, University of Göttingen, Göttingen (Germany) **1997**.
[22] J. Donohue, *The Structures of the Elements*, Wiley, New York (U.S.A.) **1974**.
[23] H. Kleinke, H. F. Franzen, *J. Solid State Chem*. **1998**, *137*, 218.
[24] P. A. Maggard, J. D. Corbett, *Inorg. Chem*. **2000**, *39*, 4143.
[25] L. Chen, J. D. Corbett, *Inorg. Chem*. **2002**, *41*, 2146.
[26] P. A. Maggard, J. D. Corbett, *J. Am. Chem. Soc*. **2000**, *122*, 838.
[27] J. Emsley, *The Elements*, Oxford University Press, Oxford, **1999**.
[28] I. Bull, V. Young, S. J. Teat, L. Peng, C. P. Grey, J. B. Parise, *Chem. Mater*. **2003**, *15*, 3818.
[29] K. Schwendtner, U. Kolitsch, *Acta Crystallogr*. **2004**, *C60*, i84.
[30] S. R. Miller, P. A. Wright, C. Serre, T. Loiseau, J. Marrot, G. Férey, *Chem. Commun*. **2005**, 3850.
[31] O. Heusler, *Ann. Phys*. **1934**, *19*, 155.
[32] E. Parthé, L. Gelato, B. Chabot, M. Penzo, K. Cenzual, R. Gladyshevskii, Gmelin Handbook of Inorganic and Organometallic Chemistry, TYPIX-*Standardized Data and Crystal Chemical Characterization of Inorganic Structure Types*, 8th ed., Springer, Berlin, **1993**.
[33] H. Hillebrecht, M. Ade, *Z. Anorg. Allg. Chem*. **1999**, *625*, 572.